Int. J. Heat Mass Transfer. Vol. 33, No. 2, pp. 331–339, 1990
Printed in Great Britain

0017–9310/90 $3.00+0.00

Turbulent Prandtl number in a circular jet

L. P. CHUA and R. A. ANTONIA
Department of Mechanical Engineering, University of Newcastle, N.S.W. 2308, Australia

(*Received* 6 *March* 1989 *and in final form* 27 *April* 1989)

Abstract—Measurements of the Reynolds shear stress and heat flux distributions at a number of streamwise stations in a heated circular jet into still air indicate that the flow is approximately self-preserving at $x/d = 15$. Measurements made with a 120° X-probe are in closer agreement with calculations obtained by integrating the mean momentum and mean enthalpy equations than measurements made with a 90° X-probe. The turbulent Prandtl number increases near the edge of the jet but, in a region between the axis and the jet half-radius, it is approximately constant (0.81 ± 0.05). This numerical value is in reasonable agreement with that selected by So and Hwang (*ZAMP* **37**, 624–631 (1986)) for similarity solutions of non-isothermal round jets. It is suggested that the early attainment of self-preservation in the present flow may be due to the laminar conditions at the jet exit.

INTRODUCTION

THERE are very few measurements for the Reynolds shear stress and heat flux in a turbulent round jet in still air. Apart from the data of Corrsin and Uberoi [1] and Chevray and Tutu [2], there is practically no information available on the turbulent Prandtl number for this flow. The scarcity of turbulence data in this flow was recently highlighted in Gouldin *et al.*'s [3] review of data in turbulent non-reacting flows. The paucity of turbulence measurements in the round jet in stagnant surroundings is, to a large extent, due to the difficulties in making accurate measurements in this flow. The two major sources of difficulty are: (i) the relatively high turbulence levels (e.g. $(\overline{u^2})^{1/2}/U$ is typically 0.25 on the axis and about 0.40 at $r = R_u$); and (ii) the likelihood of flow reversal, which increases with distance from the axis.

For high turbulence intensity flows, it has been shown [4, 5] that use of the cosine cooling law in the context of X-probe measurements can lead to quantities such as $\overline{uv}/\bar{U}^2$ and $\overline{v^2}/\bar{U}^2$ being underestimated by 8 and 17%, respectively. A dimensionless k^2 factor was introduced to complement the cosine law by taking into account the longitudinal cooling of the X-probes. However, there are difficulties in obtaining an accurate value of k^2, e.g. Jorgensen [6] and Andreopoulos [7] found that the value of k^2 varied with the yaw angle. Of equal, if not greater, importance is the validity of the implicit assumption of a constant effective angle used in the conventional method of calibrating the X-probe. Browne *et al.* [8] recently found that the wire effective angle varied with yaw angle, velocity and k^2. The concept of a constant effective angle seems therefore tenuous when the turbulence intensity is high. In ref. [8] a full velocity vs yaw angle calibration, circumventing the need to assume a specific wire cooling law, was developed. This calibration, which is similar to that originally introduced by Willmarth and Bogar [9] and subsequently developed by Johnson and Eckelmann [10], is used in the present study for the heated jet.

Difficulties associated with flow reversal can be overcome with laser Doppler velocimetry [11] or perhaps pulsed wire measurement [12, 13]. However, if information on the temperature field is required simultaneously with that on the velocity, then a X-probe/cold wire arrangement remains attractive. It was recently found that removal of part of the experimental data contaminated by flow reversal yielded nearly the same values for $\overline{uv}$ and $\overline{v\theta}$ as for the original contaminated data [14]. The reason for this is that reversal occurs mainly within non-turbulent regions of the flow. It seemed plausible that relatively reliable data could be obtained with a X-probe/cold wire arrangement.

The main aim of the present investigation is to obtain reasonably accurate Reynolds shear stress and heat flux distributions and hence a reasonably accurate determination of the turbulent Prandtl number. Another aim is to ascertain whether the early attainment of self-preservation, previously established [15] on the basis of mean velocity and mean temperature profiles as well as centreline variations of $\overline{u^2}$ and $\overline{\theta^2}$, can be extended to the Reynolds shear stress and heat flux.

Measurements were initially made with a standard 90° X-probe as most of the published data [2, 16] were made with such a probe. However, in the course of the investigation, measurements in a turbulent boundary layer over a rough wall [17, 18] indicated that the Reynolds shear stress measurement with a 120° X-probe was in closer agreement with the wall shear stress when a 90° probe was used. Browne *et al.* [19] found that a 90° X-probe can seriously underestimate the r.m.s. value of the vector cone angle β and hence $(\overline{v^2})^{1/2}$, since β may exceed 90° even on the jet axis.

NOMENCLATURE

A slope of linear variation of V_j/U_0 or T_j/T_0 vs x/d (Table 1)
d nozzle diameter [m]
d_w diameter of cold wire [m]
f dimensionless mean velocity, $\bar{U}/U_0$
f_s sampling frequency [Hz]
I_1, I_2, I_3 constants defined in equation (3)
l_w length of cold wire [m]
Pr_T turbulent Prandtl number defined by equation (7)
r radial distance from jet axis [m]
R_u half-velocity radius where $\bar{U} = U_0/2$ [m]
S magnitude of velocity vector [m s^{-1}]
$\bar{T}$ local mean temperature (relative to ambient) [K]
T_0 local mean temperature (relative to ambient) on axis [K]
u axial velocity fluctuation [m s^{-1}]
$\bar{U}$ mean axial velocity [m s^{-1}]
U_j jet exit velocity [m s^{-1}]
U_0 local mean velocity on axis [m s^{-1}]
$\overline{uv}$ kinematic Reynolds shear stress [m^2 s^{-2}]
$\bar{V}$ mean radial velocity [m s^{-1}]
v radial velocity fluctuation [m s^{-1}]
$\overline{v\theta}$ thermometric heat flux [m s^{-1} K]
w spanwise velocity fluctuation [m s^{-1}]
x axial distance from nozzle exit [m]
x_0 virtual origin [m].

Greek symbols
α temperature coefficient of resistivity [K^{-1}]
α_T turbulent diffusivity of heat defined in equation (6) [m^2 s^{-1}]
β velocity vector cone angle [deg]
η dimensionless coordinate, r/R_u
θ temperature fluctuation [K]
Θ dimensionless mean temperature, $\bar{T}/T_0$
ν_T turbulent diffusivity of momentum defined in equation (5) [m^2 s^{-1}].

Measurements were therefore repeated with a 120° X-probe for comparison with the results obtained with the standard probe.

The relative performance of the 90° and 120° X-probes can be assessed by comparing measurements of the Reynolds shear stress and heat flux with calculations made by integrating the mean momentum and mean enthalpy equations using self-preserving distributions of $\bar{U}$, $\bar{T}$, U_0, R_u and T_0.

EXPERIMENTAL TECHNIQUES

The experimental facility has been described in ref. [15]. Briefly, a variable speed centrifugal blower supplies air to an axisymmetric nozzle with a 10:1 contraction ratio. The jet is heated with 1 kW electrical coil elements distributed across the duct. The exit diameter d of the nozzle is 25.4 mm.

The velocity fluctuations, u, v and the temperature fluctuation θ were measured with a X-probe/cold wire arrangement. The X-probe was operated with DISA 55M10 constant temperature anemometers at an overheat ratio of 1.5. The 5 μm diameter (Wollaston, Pt–10% Rh) wires were etched to a nominal length of 1.2 mm. The lateral separation between wires was about 0.8 mm.

Two X-probes were used, one with an included angle between wires of about 90° and another with an angle of about 120°. These probes were calibrated for velocity and yaw in the potential core of the jet. For the 90° probe, yaw angles in the range −36° to 36° were used in 9° steps. For the 120° probe, the range was ±44° with a step of 11°. At each yaw angle, the probes were calibrated over a range of velocities covering the range expected at the measurement stations. Details of the calibration approach are given in ref. [8]. The instantaneous velocity components u and v are given by the relations $u = S\cos\beta - \bar{U}$ and $v = S\sin\beta - \bar{V}$, where the magnitude S of the velocity vector and the cone angle β are obtained directly from the full velocity vs yaw angle calibration. The calibration procedure, which is somewhat similar to the lookup table approach of Lueptow *et al.* [20], is an improvement over the constant effective angle approach, particularly for the present flow, where the turbulence intensity is high. At $x/d = 15$, $(\overline{u^2})/\bar{U}$ is 0.22 on the axis and 0.39 at $\eta = 1$.

The cold wire (0.63 μm diameter Wollaston Pt–10% Rh) was located 0.6 mm upstream of the centre of the X-probe, perpendicular to the X-probe plane. The length of the cold wire was sufficiently long ($\approx$1.8 mm) to prevent the wake behind the unetched portions of this wire from interfering with the hot wires. The cold wire was operated with a constant current circuit. The current used was 0.1 mA and the resulting sensitivity of the wire to velocity fluctuation [21] was sufficiently small ($\approx 2.8\times10^{-3}$ K (m s^{-1})$^{-1}$) to be ignored, e.g. the resulting error in the maximum value of $(\overline{u^2})^{1/2}$ would be less than 0.1% for $x/d = 15$. Using the pulsed wire technique described in ref. [22], the high frequency response of the 0.63 μm wire was estimated to be about 3.5 kHz at a velocity of 5 m s^{-1}. The length to diameter ratio ($l_w/d_w \approx 2860$) of the cold wire used is large enough to avoid any low frequency attenuation of temperature spectra due to end conduction effects [23]. Comparisons (not shown here) between the spectrum of the present cold wire and spectra measured with shorter cold wires indicated

that there was no significant high frequency attenuation for the present wire.

The temperature sensitivity ($\approx 1.69 \times 10^{-3}$ K^{-1}) of the cold wire was determined with the wire placed at the nozzle exit, using a 10 Ω platinum resistance thermometer operated in a Leeds and Northrup 8078 bridge capable of resolving 0.01 K. The jet velocity was measured with a pitot tube connected to a Furness micromanometer with a least count of 0.01 mm water. A data logger consisting of a data acquisition system (HP3497A) and a desktop computer (HP85) were used during calibration. The voltages from the wires were passed first through buck and gain circuits followed by amplifiers then through low-pass filters before they were digitized into a PDP 11/34 computer at a sampling frequency equal to f_s. The cut-off frequency of the filters was set equal to $f_s/2$. Since the high frequency end of the spectrum was not of direct interest here, the magnitude of f_s was set at a smaller value than the Kolmogorov frequency. For example, at $x/d = 15$, f_s was equal to 2500 Hz while the Kolmogorov frequency was 4000 Hz; it was estimated that this cut-off represented a loss of information for $\overline{\theta^2}$ of only 3% whereas the spectral content of fluxes $\overline{uv}$ and $\overline{v\theta}$ was fully covered. The duration of each record (typically 45 ± 5 s) was sufficient to ensure convergence of the velocity and temperature statistics. For example, at $x/d = 15$, the values of $\overline{uv}$ and $\overline{v\theta}$ at the end of 80% of the record duration were within ±5% of the final values. Measurements were made at five stations ($x/d = 15$, 20, 25, 30, 35) with a 90° X-probe, and a 120° X-probe was used to make a measurement at $x/d = 15$ for comparison with the 90° X-probe results. The measurements made with the 120° X-probe were at only one station, since the results from the 90° X-probe showed that self-preservation was achieved at $x/d = 15$. The digital data were stored on magnetic tape for processing on a VAX 8550 computer. The digitized hot wire voltages were converted to velocities, after applying a correction for the effect of air temperature changes on the heat transfer from the wires. The correction involved multiplying the wire voltages [24] by $(T_w - T_a)/(T_w - T_f)$, where T_w is the wire temperature, T_a the ambient temperature and T_f the instantaneous air temperature.

All measurements were made with a jet exit velocity U_j of 11 m s^{-1} and on a jet exit temperature, relative to ambient, of 25 K. The Reynolds number based on d is 17 700. At the nozzle exit, the boundary layer is laminar, but the mixing layer is fully turbulent at $x/d \approx 2.4$. Initial conditions, including schlieren photographs near the nozzle exit are described in ref. [15].

SELF-PRESERVATION OF VELOCITY AND TEMPERATURE INTENSITIES

Normalized mean velocity and mean temperature profiles are shown in Figs. 1 and 2, respectively, as a function of η. Both sets of profiles conform reasonably well with self-preservation. The mean temperature was measured with the X-probe switched off, since the thermal wakes from the hot wires would contaminate the cold wire signal due to flow reversal in the outer region of the jet. The results of ref. [25] indicated that flow reversal first occurs near $\eta = 0.8$. For comparison, curves of best fit to the mean velocity and mean temperature distributions measured [15] with single hot and cold wires are shown in Figs. 1 and 2. Figure 1 indicates that, although the mean velocity is adequately measured by the X-probe, the scatter is larger than that obtained with a single wire [15]. Figure 2 implies that the physical presence of the X-probe has not had any adverse effect on the mean temperature measurement. The scatter in Fig. 2 is also slightly larger than that shown in ref. [15], possibly as a result of the larger wire length ($l_w = 1.8$ mm) used here.

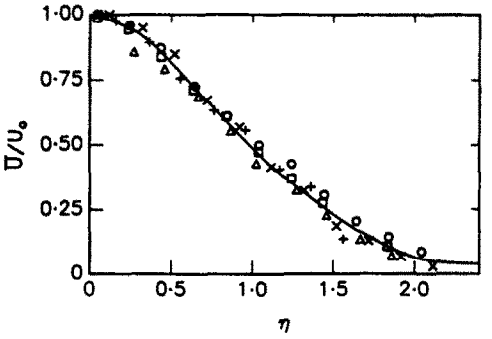

FIG. 1. Mean velocity distributions: ○, $x/d = 15$; ×, $x/d = 20$; □, $x/d = 25$; △, $x/d = 30$; +, $x/d = 35$; ——, best fit curve from ref. [15].

Axial distributions of U_0 and T_0 are shown in Fig. 3, together with the results of Corrsin and Uberoi [1], Wygnanski and Fiedler [16], Rodi [26], Hasan and Hussain [27] and Saetran [28]. In all cases the variation of U_j/U_0 or T_j/T_0 is approximately linear (except for $x/d \lesssim 6$), as required by self-preservation. There are however differences, between different investigations, in the slope A and virtual origin x_0 (Table 1) which may be due to the different initial conditions [29].

Radial distribution of $(\overline{u^2})^{1/2}/U_0$, $(\overline{v^2})^{1/2}/U_0$ and

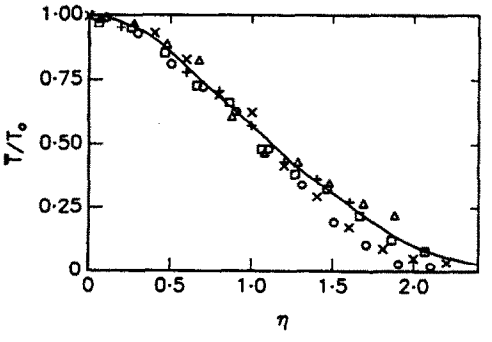

FIG. 2. Mean temperature distributions: ○, $x/d = 15$; ×, $x/d = 20$; □, $x/d = 25$; △, $x/d = 30$; +, $x/d = 35$; ——, best fit curve from ref. [15].

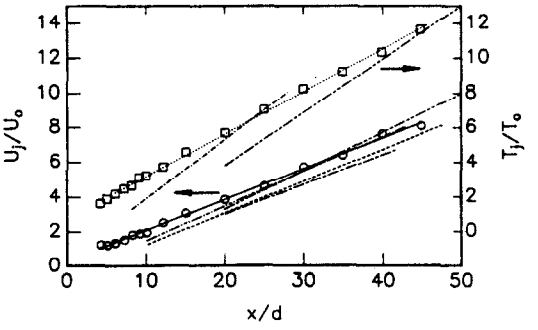

FIG. 3. Variation on the jet axis of the mean velocity U_0 and mean temperature T_0. ○, U_j/U_0; ——, best fit of ○ [present]; – – – –, Wygnanski and Fiedler [16]; — — —, Rodi [26]; — — — —, Saetran [28]; — · · —, Hasan and Hussain [27]; □, T_j/T_0; · · · · · ·, best fit of □ [present]; — — — —, Saetran [28]; — · —, Corrsin and Uberoi [1].

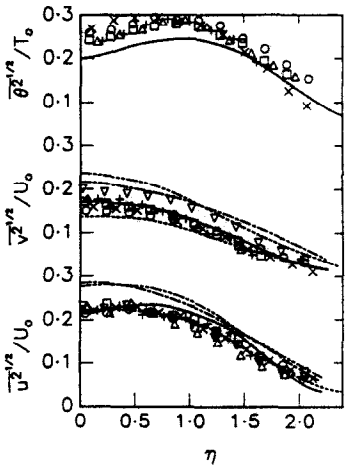

FIG. 4. Distributions of normal Reynolds stresses and temperature variance. Measurement (90° X-probe): ○, $x/d = 15$; ×, $x/d = 20$; □, $x/d = 25$; △, $x/d = 30$; +, $x/d = 35$. Measurement (120° X-probe): ▽, $x/d = 15$. ——, Chevray and Tutu [2]; – – – –, Donaldson *et al.* [30]; — — —, Rodi [26]; — — — —, Wygnanski and Fiedler [16].

$(\overline{\theta^2})^{1/2}/T_0$ are shown in Fig. 4. To within the experimental uncertainty (about ±3% for $(\overline{u^2})^{1/2}/U_0$ and $(\overline{v^2})/U_0$ and ±4% for $(\overline{\theta^2})^{1/2}/T_0$) these distributions are generally consistent with self-preservation. There are small discrepancies in the detailed distribution of $(\overline{u^2})^{1/2}/U_0$ and $(\overline{v^2})^{1/2}/U_0$ for the present results with the measurements of Chevray and Tutu [2] at $x/d = 15$ and Donaldson *et al.* [30] at $x/d = 20$. Although $(\overline{u^2})^{1/2}/U_0$, as measured with the 120° X-probe, is about the same as that obtained with the 90° X-probe, the 120° probe yields significantly larger values of $(\overline{v^2})^{1/2}/U_0$ than the 90° probe. Browne *et al.* [19] have found that the 90° probe can seriously underestimate the r.m.s. of the lateral velocity fluctuation, because the vector cone angle can exceed 90°, even on the axis of the jet.

The $(\overline{v^2})^{1/2}/U_0$ profile obtained with the 120° X-probe is in fairly good agreement with that determined by Rodi [26] who used a new method of analysing hot-wire signals. The measurements of $(\overline{v^2})^{1/2}/U_0$ obtained by Wygnanski and Fiedler [16] are much higher than the present 120° X-probe results as shown in Fig. 3. However, Rodi [26] pointed out that (i) Wygnanski and Fiedler [16] did not actually determine the value of k^2 but simply adopted Champagne *et al.*'s [4] k^2 value of 0.04 (the magnitude of $(\overline{v^2})^{1/2}$, as determined from X-wire signals, is quite sensitive to the value of k^2); and (ii) the lateral distance between the two hot wires in the X-probe of ref. [16] was very small (about 0.15 mm), making the probe very sensitive to the w component of velocity because of thermal wake effects (Jerome *et al.* [31] reported that $\overline{v^2}$, $\overline{w^2}$ and $\overline{uv}$ could be overestimated by 25%).

The difference between the present values of $(\overline{u^2})^{1/2}/U_0$ and those of Wygnanski and Fiedler or Rodi are unlikely to be due to the fact that the present x/d range is insufficient to achieve self-preservation. Indeed, the present distributions of $\overline{u^2}$, $\overline{v^2}$ and $\overline{\theta^2}$ conform with self-preservation. A more likely possibility, which requires further investigation, is that the distributions of $\overline{u^2}$, $\overline{v^2}$, $\overline{\theta^2}$, etc. are not universal but depend on the jet initial conditions. By using a more general self-preservation analysis, George [32] recently showed that there may be many self-preserving states, e.g. full, partial or local self-preservation, each of which are uniquely determined by

Table 1

Investigators	A	x_∞	Range of x/d	Nature of flow at jet exit
	(a) $U_j/U_0 = A(x/d+x_0)$			
Wygnanski and Fiedler [16]	0.169	−3.0	10–50	unspecified (probably turbulent)
Rodi [26]	0.166	−3.75	50–75	unspecified (probably turbulent)
Hasan and Hussain [27]	0.187	−3.12	10–45	laminar
Saetran [28]	0.203	−4.02	20–55	turbulent
Present	0.169	1.0	6–45	laminar
	(b) $T_j/T_0 = A(x/d+x_0)$			
Corrsin and Uberoi [1]	0.284	−2.86	8.28	unspecified
Saetran [28]	0.29	−8.23	20–55	turbulent
Present	0.23	2.28	6.45	laminar

initial conditions. The initial jet exit condition of Wygnanski and Fiedler [16] and Rodi [26] do not appear to have been specified. However, the Reynolds number was 10^5 in the former experiment and 8.7×10^4 for the latter experiment. At these Reynolds numbers, significantly larger than the present Reynolds number, exit conditions are likely to be turbulent in contrast with the present laminar exit condition.

The interaction region of a circular jet into still air was found to be short and weaker than for a plane jet with laminar initial conditions [15]. Possibly because of the short and weak interaction region of the present jet, self-preservation is achieved quickly. Hill *et al.* [33] showed that jets (both plane and circular) with laminar initial boundary layers were found to have faster mixing rates, a much more prominent large-scale structure and a more rapid centreline velocity decay than those with an initially turbulent boundary layer. The early attainment of self-preservation is useful from an experimental viewpoint as it avoids having to make measurements at large streamwise distances where the accuracy of measurement is small. From a modelling viewpoint turbulent initial conditions may be preferable, since they avoid including transition in the calculation domain, e.g. Gouldin *et al.* [3].

MEASUREMENTS AND CALCULATION OF REYNOLDS SHEAR STRESS AND HEAT FLUX

Distributions of the Reynolds shear stress (Fig. 5) and heat flux (Fig. 6) also conform with self-preservation. The scatter in $\overline{v\theta}/U_0T_0$ is slightly larger than $\overline{uv}/U_0^2$, especially in the outer jet region, which may be due to the larger scatter of $(\overline{\theta^2})^{1/2}/T_0$ (see Fig. 4) in the same region. The experimental uncertainty for the heat flux is about $\pm 14\%$ ($\pm 12\%$ for the 120° X-probe), compared with about $\pm 12\%$ ($\pm 10\%$ for the 120° X-probe) for the Reynolds shear stress. These uncertainties are estimated from the scatter of the experimental data obtained with the 90° X-probe at five different streamwise stations and the repeated

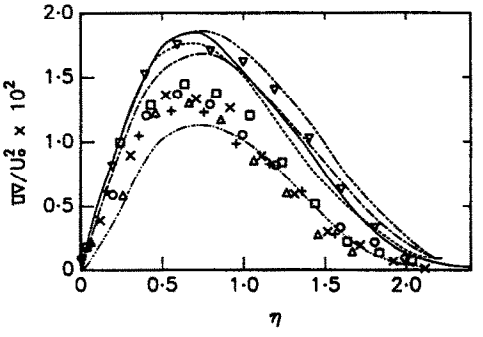

FIG. 5. Reynolds shear stress distributions. 90° X-probe: ○, $x/d = 15$; ×, $x/d = 20$; □, $x/d = 25$; △, $x/d = 30$; +, $x/d = 35$. — · — · —, Chevray and Tutu [2]. 120° X-probe: ▽, $x/d = 15$. Calculations: ——, present, relation (1); — — —, Rodi [26] (with normal stress terms); — — —, Rodi [26] (no normal stress terms); – – –, So and Hwang [37].

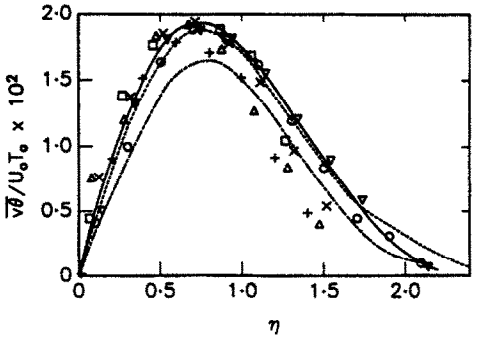

FIG. 6. Heat flux distributions. Measurement (90° X-probe): ○, $x/d = 15$; ×, $x/d = 20$; □, $x/d = 25$; △, $x/d = 30$; +, $x/d = 35$. — — —, Chevray and Tutu [2]. Measurement (120° X-probe): ▽, $x/d = 15$. Calculations: ——, present, relation (2); – – –, So and Hwang [37].

experimental data for the 120° X-probe at $x/d = 15$. The scatter is generally larger for $\eta > 1$ than $\eta < 1$. The large magnitude of the uncertainty is most probably due to the high local turbulence intensity (e.g. at $x/d = 15$, $(\overline{u^2})^{1/2}/\bar{U}$ exceeds 0.4 when η is larger than 1.0) rather than to flow reversal. It was recently found that the removal of data affected by flow reversal does not change the Reynolds shear stress and the average heat flux significantly since flow reversal coincides, with high probability, with non-turbulent periods and occurs for only a small fraction of time for which the flow is non-turbulent [14].

Apart from the rectification error associated with flow reversal, the X-wire may be adversely affected by the influence of the transverse (w) velocity fluctuation. Tutu and Chevray [34] found that when rectification errors are large, so are those caused by large w fluctuations. By comparing the standard X-probe signals with computer simulated Gaussian velocity signals, Kawall *et al.* [35] were able to assess the importance of several factors, including w, in addition to the rectification error, that can affect the hot wire performance. Their results indicate that w cause $(\overline{v^2})^{1/2}$ to be underestimated by a maximum of about 14% for $(\overline{u^2})^{1/2}/\bar{U} = 80\%$ and $\overline{uv}$ by about 16% for $(\overline{u^2})^{1/2}/\bar{U} = 30\%$. The error in $(\overline{u^2})^{1/2}$ is generally less than 2% over the range $15\% \leqslant (\overline{u^2})^{1/2}/\bar{U} \leqslant 80\%$. Since Kawall *et al.*'s [35] analysis (a similar analysis was carried out by Tutu and Chevray [34]) is based on a constant effective angle calibration approach, the relevance of the above estimates to the present experiments, which use a full velocity vs yaw angle approach, is qualitative rather than quantitative. The trend of Kawall *et al.*'s [35] results is similar to the present observation that the 120° X-probe yields larger values of $(\overline{v^2})^{1/2}/U_0$ and $\overline{uv}/U_0^2$ but not $(\overline{u^2})^{1/2}/U_0$ than the 90° X-probe (Figs. 4 and 5). For these reasons and because the effect of w may be smaller on the 120° X-probe than on the standard X-probe, no w corrections have been applied to the present 120° X-probe data.

The distributions of $\overline{uv}/U_0^2$ and $\overline{u\theta}/U_0T_0$ are in

reasonable agreement with those of Chevray and Tutu [2]. The present peak values of $\overline{uv}/U_0^2$ and $\overline{v\theta}/U_0T_0$ occur at $\eta \approx 0.7$, compared with $\eta \approx 0.8$ for Chevray and Tutu. The inequality $\overline{v\theta}/U_0T_0 > \overline{uv}/U_0^2$, which Chevray and Tutu associated with a higher efficiency for heat transfer relative to momentum transfer, also applies to the present data.

The calculated distributions of $\overline{uv}/U_0^2$ and $\overline{v\theta^2}/U_0T_0$, inferred from the momentum and enthalpy equations as well as the measured mean velocity and mean temperature profiles, are shown in Figs. 5 and 6. The details of these calculations can be found in ref. [29]. The final expressions are written below

$$\frac{\overline{uv}}{U_0^2} = \left(2\frac{dR_u}{dx} + \frac{R_u}{U_0}\frac{dU_0}{dx}\right)\frac{f}{\eta}I_1 - \left(2\frac{dR_u}{dx} + 2\frac{R_u}{U_0}\frac{dU_0}{dx}\right)\frac{I_2}{\eta} \quad (1)$$

and

$$\frac{\overline{v\theta}}{U_0T_0} = -\left[\frac{R_u}{T_0}\frac{dT_0}{dx} + 2\frac{dR_u}{dx} + \frac{R_u}{U_0}\frac{dU_0}{dx}\right)\frac{I_3}{\eta} + \left(2\frac{dR_u}{dx} + \frac{R_u}{U_0}\frac{dU_0}{dx}\right)\frac{\Theta}{\eta}I_1 \quad (2)$$

where

$$f(\eta) = \frac{\bar{U}}{U_0}; \quad \Theta(\eta) = \frac{\bar{T}}{T_0}; \quad I_1 = \int_0^\eta f\eta\, d\eta;$$

$$I_2 = \int_0^\eta f^2\eta\, d\eta \quad \text{and} \quad I_3 = \int_0^\eta f\Theta\eta\, d\eta. \quad (3)$$

The assumption of self-preservation has been used in equations (1) and (2); the normal stresses have not been included in equation (1) while viscous diffusion terms have been neglected in both equations (1) and (2). Rajaratnam [36] noted that the viscous diffusion could be neglected if the Reynolds number is greater than a few thousand. The streamwise variations of dR_0/dx, dU_0/dx and dT_0/dx, determined in ref. [15], were substituted in equations (1) and (2).

The values of $\overline{uv}/U_0^2$ measured with the 120° X-probe are larger than those obtained with the 90° X-probe and in closer agreement with equation (1). It was shown in ref. [19] that the 90° probe can seriously underestimate the magnitude of $\overline{uv}$ because the vector cone angle can exceed 90°, even on the jet axis. As shown in Fig. 4 (see also Kawall *et al.* [35]), v is the quantity which is most affected while u is practically unaffected. One would therefore expect $\overline{v\theta}$ to be affected, although perhaps not quite to the same extent as $\overline{uv}$. However, this is not supported by the data since the 90° X-probe values of $\overline{v\theta}$ are generally in reasonable agreement with those from the 120° X-probe and those determined from relation (2). The early attainment of self-preservation for the present circular jet with laminar initial conditions, was further confirmed by the reasonable agreement between the calculated shear stress and heat flux distribution and measurements with a 120° X-probe at $x/d = 15$.

Rodi's calculations [26] (with and without normal stress terms) are also presented in Fig. 5. The peak of the present calculation is in reasonable agreement with the peak value of Rodi's calculation which includes normal stresses. In the outer part of the jet, it is in closer agreement with Rodi's calculation in the absence of normal stress terms. Rodi's calculation with normal stress terms may overestimate the Reynolds shear stress; his measurements are smaller than the calculation (see Fig. 13 of ref. [26]) for $\eta \geqslant 1.2$. Rodi's equation is reproduced below as equation (4). The larger values of Reynolds stress obtained by Rodi's equation may be attributed to the normal stress terms which contributed about 10% to the shear stress

$$\frac{\overline{uv}}{U_0^2} = \frac{\bar{U}/U_0}{r/x}\int_0^{r/x}\frac{\bar{U}}{U_0}\frac{r}{x}\,d(r/x) + \frac{r}{x}\left(\frac{\overline{u^2}}{U_0^2} - \frac{\overline{v^2}}{U_0^2}\right). \quad (4)$$

Departing from Tollmien's classical treatment of assuming a constant eddy viscosity, So and Hwang [37] obtained a family of similarity solutions for normalized mean velocity and mean temperature, eddy viscosity, Reynolds shear stress and heat flux in the case of a heated circular jet. The distributions of $\overline{uv}/U_0^2$ and $\overline{v\theta}/U_0T_0$ of ref. [37] are plotted in Figs. 5 and 6, respectively. The present results are higher than those of ref. [37], except at large η, and the discrepancy is larger for $\overline{uv}/U_0^2$ than $\overline{v\theta}/U_0T_0$.

EDDY DIFFUSIVITIES AND TURBULENT PRANDTL NUMBER

The eddy diffusivities are given by

$$\nu_T = -\frac{\overline{uv}}{(\partial\bar{U}/\partial r)} \quad (5)$$

and

$$\alpha_T = -\frac{\overline{v\theta}}{(\partial\bar{T}/\partial r)}. \quad (6)$$

The turbulent Prandtl number Pr_T defined as the ratio of eddy diffusivities for momentum and heat can be written as

$$Pr_T = \frac{\nu_T}{\alpha_T}. \quad (7)$$

The calculated distributions of ν_T/U_0R_u and α_T/U_0R_u are plotted in Figs. 7 and 8, respectively. The limiting values of these two quantities at $\eta = 0$ are determined from l'Hôpital's rule. The calculated eddy viscosity is in good agreement with measurements made with the 120° X-probe. The self-preserving eddy viscosity distribution of So and Hwang (equations (7) and (23) in their paper) is also plotted in Fig. 7. Their ν_T distribution is in general agreement with the present

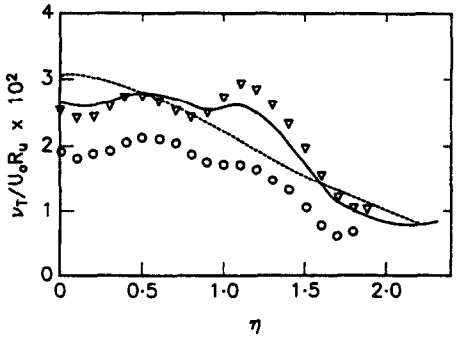

FIG. 7. Turbulent momentum diffusivity. Measurement (90° X-probe): ○, $x/d = 15$. Measurement (120° X-probe): ▽, $x/d = 15$. Calculations: ——, present; – – –, So and Hwang [37].

calculation and measurements made with the 120° X-probe.

As shown in Fig. 8 the calculated turbulent thermal diffusivity α_T/U_0R_u and the measurements made with 90° and 120° X-probes are in good agreement except for small discrepancies near the axis. For $\eta \leqslant 0.3$, the calculated α_T distribution shows a larger variation than the ν_T distribution. However, both distributions indicate that α_T and ν_T may be assumed constant for $0.1 \leqslant \eta \leqslant 1.0$.

Calculated and measured distributions of Pr_T are shown in Fig. 9. It is evident that measurements with the 120° X-probe are in closer agreement with the calculation than those from 90° X-probes. However, all three distributions show similar trends. Using l'Hôpital's rule at $\eta = 0$, Pr_T was found to be equal to 3 for the calculation, 2.4 for the 90° X-probe data and 3.6 for the 120° X-probe data. Pr_T increases near the axis and near the jet edge. Elsewhere, there are oscillations with local maxima at $\eta \approx 0.5$ and 1.2 and minima at $\eta \approx 0.3$, 0.84 and 1.6 (these local fluctuations could be reproduced within the range of uncertainties given below). The experimental uncertainty in Pr_T was estimated, by the method of propagation of errors [38], from uncertainties in $\overline{uv}/U_0^2$, $\overline{v\theta}/U_0T_0$, $\partial\bar{U}/\partial y$ (about $\pm 3\%$) and $\partial\bar{T}/\partial y$ (about $\pm 3\%$) is approximately equal to ± 16 and $\pm 19\%$ for the 120° and 90° probes, respectively. The distributions of Pr_T for Corrsin and Uberoi [1] and

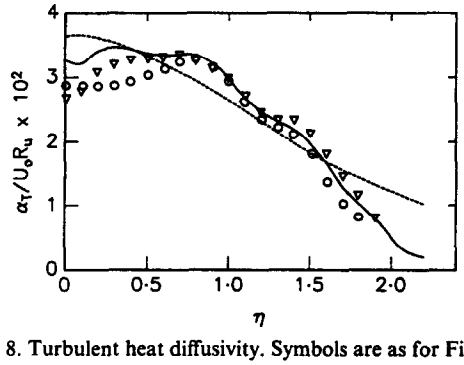

FIG. 8. Turbulent heat diffusivity. Symbols are as for Fig. 6.

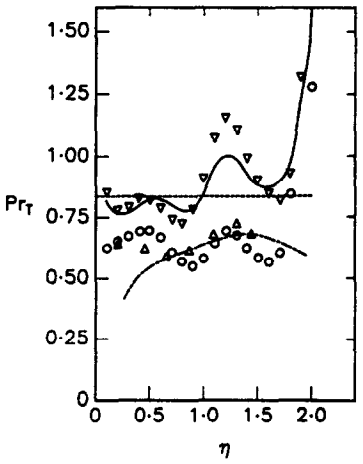

FIG. 9. Turbulent Prandtl number Pr_T. △, Corrsin and Uberoi [1]; – – –, Chevray and Tutu [2]. Other symbols are as for Fig. 6.

Chevray and Tutu [2] are at about the same level with the present 90° X-probe measurement, these results indicated the limitations of measurements made with 90° X-probes for the present high turbulence intensity flow.

Neither the calculated nor the measured Prandtl number distribution suggests that Pr_T can be assumed constant across the whole jet. However, in the range $0.1 \leqslant \eta \leqslant 1.0$, Pr_T is reasonably constant with an average value of 0.81 (for both the calculation and measurements with the 120° X-probe), which is in reasonable agreement with the value of 0.84 assumed by So and Hwang [37] in determining the mean temperature and heat flux profiles. Accordingly, the turbulent diffusivity of heat α_T from the results of ref. [37] was inferred using $\alpha_T = \nu_T/Pr_T$ with $Pr_T = 0.84$ and plotted in Fig. 8 along with the present results. There are no significant differences between the distributions for $\eta \leqslant 1.6$.

CONCLUSIONS

The measured distributions of Reynolds stresses, temperature intensities and heat fluxes suggest that, for the present round jet into still air, self-preservation is attained at approximately 15 diameters downstream of the nozzle. This short distance is consistent with the short interaction region for this flow, as established in an earlier study [15]. The laminar boundary layer at the exit of the present jet is probably responsible for the early attainment of self-preservation but a systematic study of the effect of initial conditions is required before a definite statement can be made.

The 90° and 120° X-probes yield approximately the same heat flux distribution but the Reynolds shear stress measured by the 120° X-probe is significantly larger than that of the 90° X-probe and in closer agreement with the calculation based on the mean momentum and mean enthalpy equations. As a result, the turbulent Prandtl number obtained from

the 120° X-probe data is larger (by about 30%) than that determined by the 90° X-probe.

One implication of the present measurements is that the Reynolds shear stress and the heat flux can be estimated with acceptable accuracy with a X-probe/cold wire arrangement provided the geometry and calibration of the X-probe are designed to account for the large excursions of the velocity vector in the plane of the probe. In the outer part of the jet, reversal occurs mainly when the flow is non-turbulent [14] so that the Reynolds shear stress and heat flux data from the present arrangement should be sufficiently accurate.

Over the range $0.1 \leqslant \eta \leqslant 1$, the turbulent Prandtl number may be considered to be approximately constant (0.81 ± 0.05). Its magnitude supports the value selected by So and Hwang [37] in their proposed similarity solutions of a non-isothermal round jet.

REFERENCES

1. S. Corrsin and M. S. Uberoi, Further investigations on the flow and heat transfer in a heated turbulent air jet, NACA Report 998 (1950).
2. R. Chevray and N. K. Tutu, Intermittency and preferential transport of heat in a round jet, *J. Fluid Mech.* **88**, 133–160 (1978).
3. F. C. Gouldin, R. W. Schefer, S. C. Johnson and W. Kollmann, Nonreacting turbulent mixing flows, *Prog. Energy Combust. Sci.* **12**, 257–303 (1986).
4. F. H. Champagne, C. A. Sleicher and O. H. Wehrmann, Turbulence measurements with inclined hot-wires. Part I: heat transfer measurements with inclined hot-wires, *J. Fluid Mech.* **28**, 153–175 (1967).
5. F. H. Champagne and C. A. Sleicher, Turbulence measurements with inclined hot-wires. Part II: hot-wires response equations, *J. Fluid Mech.* **28**, 177–182 (1967).
6. F. E. Jorgensen, Directional sensitivity of wire and fibre-film probes, *DISA Inf.* **11**, 31–37 (1970).
7. J. Andreopoulos, Improvements of the performance of triple hot wire probes, *Rev. Scient. Instrum.* **54**, 733–740 (1983).
8. L. W. B. Browne, R. A. Antonia and L. P. Chua, Calibration of X-probes for turbulent flow measurements, *Exps Fluids* **7**, 201–208 (1989).
9. W. W. Willmarth and T. J. Bogar, Survey and new measurements of turbulent structure near the wall, *Physics Fluids* S9–S21 (1977).
10. F. D. Johnson and H. Eckelmann, A variable angle method of calibration for X-probes applied to wall-bounded turbulent shear flow, *Exps Fluids* **2**, 121–130 (1984).
11. F. Durst, A. Melling and J. H. Whitelaw, *Principles and Practice of Laser-Doppler Anemometry*. Academic Press, New York (1976).
12. L. J. S. and Bradbury and I. P. Castro, A pulsed-wire technique for velocity measurements in highly turbulent flows, *J. Fluid Mech.* **49**, 657–691 (1971).
13. M. Jaroch, Development and testing of pulsed-wire probes for measuring fluctuating quantities in highly turbulent flows, *Exps Fluids* **3**, 315–322 (1985).
14. L. P. Chua and R. A. Antonia, Flow reversal and intermittency of a turbulent jet, *AIAA J.* **27**, 1494–1499 (1990).
15. L. P. Chua and R. A. Antonia, The turbulent interaction region of a circular jet, *Int. Commun. Heat Mass Transfer* **13**, 545–558 (1986).
16. I. Wygnanski and H. Fiedler, Some measurements in the self-preserving jet, *J. Fluid Mech.* **38**, 577–612 (1969).
17. M. Acharya and M. P. Escudier, Turbulent flow over mesh roughness. In *Turbulent Shear Flows V*, pp. 176–185. Springer, Berlin (1987).
18. A. E. Perry, K. L. Lim and S. M. Henbest, An experimental study of the turbulence structure in smooth- and rough-wall boundary layers, *J. Fluid Mech.* **177**, 437–466 (1987).
19. L. W. B. Browne, R. A. Antonia and L. P. Chua, Velocity vector cone angle in turbulent flows, *Exps Fluids* **8**, 13–16 (1990).
20. R. M. Lueptow, K. S. Breuer and J. H. Haritonidis, Computer aided calibration of X-probes using a lookup table, *Exps Fluids* **6**, 115–118 (1988).
21. J. C. Wyngaard, The effect of velocity sensitivity on temperature derivative statistics in isotropic turbulence, *J. Fluid Mech.* **48**, 763–768 (1971).
22. R. A. Antonia, L. W. B. Browne and A. J. Chambers, Determination of time constants of cold wires, *Rev. Scient. Instrum.* **52**, 1382–1385 (1981).
23. L. W. B. Browne and R. A. Antonia, The effect of wire length on temperature statistics in a turbulent wake, Report T.N. FM 85/7, Department of Mechanical Engineering, University of Newcastle, Australia (1985).
24. P. Bradshow, *An Introduction to Turbulence and its Measurement*. Pergamon Press, Oxford (1975).
25. R. A. Antonia, A. J. Chambers and A. K. M. F. Hussain, Errors in simultaneous measurements of temperature and velocity in the outer part of a heated jet, *Physics Fluids* **23**, 871–874 (1980).
26. W. Rodi, A new method of analysing hot-wire signals in highly turbulent flow, and its evaluation in a round jet, *DISA Inf.* **17**, 9–18 (1975).
27. M. A. Z. Hasan and A. K. M. F. Hussain, The self-excited axisymmetric jet, *J. Fluid Mech.* **115**, 59–89 (1982).
28. L. R. Saetran, Experimental investigation and mathematical modelling of momentum, heat and mass transport in some turbulent flows, Ph.D. Thesis, University of Trondheim, Norway (1984).
29. J. O. Hinze, *Turbulence* (2nd Edn). McGraw-Hill, New York (1975).
30. C. D. Donaldson, R. S. Snedeker and D. P. Margolis, A study of free jet impingement. Part 2: free jet turbulent structure and impingement heat transfer, *J. Fluid Mech.* **45**, 477–512 (1971).
31. F. E. Jerome, D. E. Guitton and R. P. Patel, Experimental study of the thermal wake interference between closely spaced wires of a X-type hot-wire probe, *Aeronaut. A.* 119–126 (May 1971).
32. W. K. George, The self-preservation of turbulent flows and its relation to initial conditions and coherent structures. In *Advances in Turbulence* (Edited by R. E. A. Arndt and W. K. George). Horizon (1988).
33. W. J. Hill, Jr., R. C. Jenkins and B. L. Gilbert, Effects of the initial boundary-layer state on turbulent jet mixing, *AIAA J.* **14**, 1513–1514 (1976).
34. N. K. Tutu and R. Chevray, Cross-wire anemometry in high intensity turbulence, *J. Fluid Mech.* **71**, 785–800 (1975).
35. J. G. Kawall, M. Shokr and J. F. Keffer, A digital technique for the simultaneous measurement of streamwise and lateral velocities in turbulent flows, *J. Fluid Mech.* **133**, 83–112 (1983).
36. N. Rajaratnam, *Turbulent Jets*, Vol. 5. Elsevier, Amsterdam (1976).
37. R. M. C. So and B. C. Hwang, On similarity solutions for turbulent and heated round jets, *ZAMP* **37**, 624–631 (1986).
38. S. J. Kline and F. A. McClintock, Describing uncertainties in single-sample experiments, *Mech. Engng* **75**, 3–19 (1953).

NOMBRE DE PRANDTL TURBULENT DANS UN JET CIRCULAIRE

Résumé—Des mesures de tensions de Reynolds et de distribution de flux thermiques dans plusieurs sections droites d'un jet chaud circulaire dans l'air au repos montre que l'écoulement est approximativement en auto-préservation à $x/d = 15$. Des mesures faites avec une sonde 120° en X sont en accord étroit avec des calculs faits en intégrant les équations de quantité de mouvement et d'enthalpie moyennes à partir de mesures effectuées avec une sonde X à 90°. Le nombre de Prandtl turbulent augmente près du bord du jet mais il est à peu près constant ($0{,}81 \pm 0{,}05$) entre l'axe et le demi-rayon du jet. Cette valeur numérique est raisonnablement en accord avec celle qui est donnée par So et Hwang (*ZAMP* 37, 624–631 (1986)) pour des solutions affines de jets ronds non isothermes. On suggère que l'apparition anticipée de la self-préservation dans le présent écoulement peut être due aux conditions laminaires à la sortie du jet.

TURBULENTE PRANDTL-ZAHL IN EINEM KREISRUNDEN STRAHL

Zusammenfassung—Es wird über Messungen der Verteilung von Schubspannung und der Wärmestromdichte entlang eines beheizten kreisrunden Strahls in ruhender Luft berichtet. Es zeigt sich, daß die Strömung für ungefähr $x/d = 15$ selbsterhaltend ist. Die Integration der Mittelwertgleichungen für Impuls und Enthalpie zeigt eine bessere Übereinstimmung mit Messungen, die mit einem 120° X-Fühler ausgeführt wurden als solche mit einem 90° X-Fühler. Die turbulente Prandtl-Zahl nimmt in Randnähe des Strahls zu und ist im Gebiet zwischen der Achse und dem halben Radius ungefähr konstant ($0{,}81 \pm 0{,}05$). Dieser numerisch ermittelte Wert zeigt eine befriedigende Übereinstimmung mit den von So und Hwang (*ZAMP* 37, 624–631 (1986)) ermittelten Lösung für den nicht-isothermen kreisrunden Strahl. Es wird vermutet, daß das frühzeitige Erreichen der Selbsterhaltung im vorliegenden Fall auf die laminare Strömung am Düsenaustritt zurückzuführen ist.

ТУРБУЛЕНТНОЕ ЧИСЛО ПРАНДТЛЯ ДЛЯ ТЕЧЕНИЯ В КРУГЛОЙ ТРУБЕ

Аннотация—Измерения распределений рейнольдсовского напряжения сдвига и теплового потока в большом числе точек, расположенных по течению нагретой круглой струи, истекающей в неподвижный воздух, показывают, что течение является приблизительно самосохраняющимся при $x/d = 15$. Измерения, проведенные с использованием 120-градусного X-образного датчика, лучше согласуются с расчетами, полученными методом интегрирования уравнений среднего количества движения и средней энтальпии, чем измерения, выполненные при помощи 90-градусного X-образного датчика. Турбулентное число Прандтля возрастает вблизи края струи, однако в области между осью и полурадиусом струи оно является приблизительно постоянным ($0{,}81 \pm 0{,}05$). Данное числовое значение удовлетворительно согласуется с числовым значением, выбранным Со и Хвангом (*ZAMP* 37, 624–631 (1986)) для автомодельных решений неизотермических круглых струй. Предполагается, что раннее достижение самосохранения данным потоком обусловлено ламинарным условием на выходе из струи.